Assessment of reactive surface and kinetic parameters of basaltic rocks as CO_2 storage

Karin Kauss[1,2], Ronald Mejia[1], Deane Roehl[1,2]

[1]*Tecgraf Institute, Pontifical Catholic University of Rio de Janeiro, 22451-000, RJ, Brazil.*

karinkauss@tecgraf.puc-rio.br, rmejias@tecgraf.puc-rio.br

[2]*Department of Civil and Environmental Engineering - Pontifical Catholic University of Rio de Janeiro*

Rua Marques de São Vicente, 225, 22451-900, 22451-900, Gávea, Rio de Janeiro – RJ.

karinkauss@tecgraf.puc-rio.br, deane@tecgraf.puc-rio.br

Abstract. Carbon Capture and Storage (CCS) is a novel technology that aims to reduce the presence of carbon dioxide in the atmosphere. This technology involves capturing CO_2 from industrial sources or directly from the air, treating, transporting, and long-term storing it in safe rock formations. Basaltic rock comprises reactive minerals and glassy phases, which trap CO_2 permanently through the mineralization mechanism. Mineralization occurs at the interface between the reactive fluid and the basaltic rock surface, converting the dissolved CO_2 into solid carbonate mineral that precipitates in the pores and fractures of the rock matrix. However, the role of the kinetics parameters in the reaction rate of minerals in basalt formations is still a developing area of research. This work investigates the influence of parameters such as temperature, CO_2 pressure, and porosity on the reaction rate of basaltic rocks. The geochemical software PHREEQC is used to explore the performance of basaltic rock dissolution and precipitation, utilizing the Carbfix library to simulate the batch reactor procedure. The numerical results address the potential of basaltic rock for CO_2 mineral storage as solid carbonates and identify the main factors that limit or improve the mineralization process.

Keywords: CO_2 mineralization, carbon capture and storage, mineralization, reaction rate, basaltic rocks.

1 Introduction

Since 2022, atmospheric CO_2 levels have soared, reaching 407 ppm in 2018, significantly higher than the pre-industrial level of 280 ppm. This rapid increase, approximately 2.3 ppm annually over the past decade, is a hundred times faster than natural rates [1]. The main cause is fossil fuel usage, which increases the greenhouse effect and global warming. Carbon Capture and Storage (CCS) appears as an innovative solution involving the promotion of a significant and continuous reduction in the net amount of CO_2 released into the atmosphere [2][3]. CCS involves a range of processes: capturing, separating, transporting, storing, and monitoring CO_2. Recently, several studies have demonstrated the feasibility of CO_2 storage using different trapping mechanisms, such as structural, residual, solubility, and mineral traps. The mineral trap is considered the most stable mechanism because it injects CO_2 into highly reactive rock formations, such as basalt, which reacts with minerals to form stable carbonate products [4]. Basalt, with its reactive minerals and glassy phases, is ideal for this process [2]. The complexity of mineralization arises from the rapid interaction between solid and liquid phases [5], while the reaction rate of basaltic rock is heavily influenced by factors such as CO_2 wettability and rock-fluid interactions [6]. Basalts have demonstrated remarkable CO_2 absorption capacity and typically form 6-7 km thick layers, maintaining consistent stratigraphy globally [7].

Geochemical environments vary significantly with location and depth, leading to alterations in the rock matrix and changes in the petrophysical properties of basalt [8]. Carbon dioxide (CO_2) solved in a fluid such as water and brine naturally reacts with mafic and ultramafic rock, creating great interest due to the carbon dioxide storage potential [9]. Basalt is also known to consume CO_2 through various natural processes, such as CO_2

metasomatism, which facilitates extensive interactions between CO_2, water, and basalt [10]. In the carbon capture process, CO_2 is introduced into basalt directly or after being dissolved in water [7]. This process triggers a series of reactions where CO_2 dissolves in water, forming carbonic acid, equation set 1 [6], whose properties vary with pressure, temperature, and salinity. Carbonic acid then reduces the pH of the in-situ water, increasing its reactivity. This high reactivity causes H^+ ions to interact with basalt glass, dissolving primary minerals in the rock matrix. As a result, divalent cations (Ca^{2+}, $Mg^{2+}$and Fe^{2+}) are released into the solution, equation set 2 [4]. These released cations subsequently react with dissolved CO_2, forming stable carbonate minerals such as calcite ($CaCO_3$), magnesite ($MgCO_3$), and siderite ($FeCO_3$), equation set 3 [11].

Dissolution CO_2

$$CO_{2(g)} + H_2O \leftrightarrow H_2CO_3$$
$$H_2CO_3 \leftrightarrow HCO_3^- + H^+ \quad (1)$$

Mineral Dissolution

$$Basaltic\ Glass + xH^+ \rightarrow 2Mg^{2+} + Ca^{2+} + Fe^{2+} + SiO_{2(aq)} \ldots$$
$$Mg_2SiO_4 + 4H^+ \rightarrow 2Mg^{2+} + 2H_2O + SiO_{2(aq)} \quad (2)$$
$$Fe_2SiO_4 + 4H^+ \rightarrow 2Fe^{2+} + 2H_2O + SiO_{2(aq)}$$

Precipitation form carbonates

$$(Mg, Fe, Ca)^{2+} + CO_3^- \rightarrow (Mg, Fe, Ca)CO_3 \quad (3)$$

Large-scale CO_2 mineralization occurs naturally in various environments by injecting CO_2 into a potential source of a divalent metal, such as basalt rock. The divalent metal is required for the carbonation phenomenon [4]. The minerals that makeup basalt, the most efficient for carbon capture, are forsterite, wollastonite, serpentine, anorthite, and basaltic glass [12]. Table 1 shows the potential sources of divalent metal. On the other hand, carbonates are more stable rocks with a high potential to store CO_2, allowing long-term storage [13]. Table 2 shows the potential CO_2 mineral hosts.

Table 1. Potential minerals for carbon mineralization (Oelkers, Gislason, and Matter, 2008)

Solid	Chemical Formula	Tons required to sequester 1 ton of carbon
Wollastonite	$CaSiO_3$	9.68 as calcite
Forsterite	Mg_2SiO_4	5.86 as magnesite
Serpentine/ chrysotile	$Mg_3Si_2O_5(OH)_4$	7.69 as magnesite
Anorthite	$CaAl_2Si_4O_8$	23.1 as calcite
Basaltic glass	$Na_{0.08}K_{0.08}Fe(II)_{0.17}Mg_{0.28}Ca_{0.26}$ $Al_{0.36}Fe(III)_{0.02}SiTi_{0.02}O_{3.45}$	8.67 as Calcite Mg as Magnesite Fe as Siderite

Table 2. Carbonate phases for potential mineral storage of CO_2 (Oelkers, Gislason, and Matter, 2008)

Mineral	Chemical Formula	Mass produced per ton C (ton)	Volume produced per ton C (m^3)
Calcite	$CaCO_3$	8.34	3.08
Magnesite	$MgCO_3$	7.02	2.36
Dawsonite	$NaAl(CO_3)(OH)_2$	12.00	4.95
Siderite	$FeCO_3$	9.65	2.49
Ankerite	$Ca(Fe, Mg)(CO_3)_2$	8.60	2.81

Recognizing the importance and complexity of CO_2 mineralization, this work focuses on CO_2 mineralization in basaltic rocks and the precipitation of carbonates and secondary phases under various initial conditions (temperature, CO_2 pressure, and pH) using 1D numerical simulation in a batch reactor. The numerical results are validated against available results in the literature. As a result, it also indirectly validates the applicability of the Carbfix database to various basaltic rocks other than those extracted at Carbfix sites. Finally, a sensitivity analysis was conducted to understand the influence of critical parameters, such as pH, temperature, and constant CO_2 pressure, on the reaction rate of basaltic rock dissolution. These factors have been proven to affect the efficiency of CO_2 mineralization.

2 Methodology

The numerical simulations were performed with PHREEQC, a versatile geochemical modeling code capable of simulating complex thermodynamic models of interactions between dissolved gases, aqueous solutions, and mineral assemblages in batch systems [14]. Since PHREEQC can only model fully saturated systems, natural conditions must be simplified to end-member scenarios. The simulation represents the basalt alteration in the H_2O-rich phase at constant CO_2 pressure. The validity of such models critically depends on the accuracy of the thermodynamic database used. All simulations use the carbfix.dat database, which improves the core10.dat resources by incorporating the reactive rate equation into a PHREEQC script to model fluid-rock interactions during mineral-hosted carbonation efforts [15][16]. Dissolution rates of minerals in the basaltic rock were calculated according to the following kinetic equation,

$$r_+ = S\left\{k_H\, exp\left(\frac{-E_{a,H}}{RT}\right) a_H^{nH} + k_N\, exp\left(\frac{-E_{a,N}}{RT}\right) + k_{OH}\, exp\left(\frac{-E_{a,OH}}{RT}\right)\right\}\left(1 - exp\left(\frac{\Delta G_r}{RT}\right)\right) \quad (4)$$

where S is the reactive surface area (m^2), k_i are rate constants (moles/m^2.s), a_H is the H^+ activity, n is the reaction order with respect to H^+ and OH^-, ΔG_r is the Gibbs free energy of the reaction, R is the gas constant, T is the absolute temperature. Reaction rate constants for crystalline basalt (pyroxenes and plagioclase) and pH dependencies were obtained from Heřmanská et al., 2022. The dissolution rate of basaltic glass was calculated according to the expression suggested in Equation 6. The reactive surface area, S_i, was calculated according to Equation 7 using the specific surface area for basalt S_{sp} as 1.52×10^{-5} m^2/g, where M is the molar mass (see Table 3), and n is the number of moles of mineral i. Also, X_r is the fraction of the total mineral surface that is reactive. As X_r defines the reactivity probability of the mineral grain, commonly used as 1 in many references such as [17].

$$r_+ = k_+ exp\left(\frac{-E_a}{RT}\right) S\left(\frac{a_{H^+}^3}{a_{Al^{3+}}}\right)^{0.33}\left(1 - exp\left(\frac{\Delta G_r}{RT}\right)\right) \quad (6)$$

$$S_i = M_i n_i S_{sp} X_r \quad (7)$$

The basalt was defined as a mixture of glass and crystalline basalt with minerals. In this study, the simulations were conducted using a basaltic rock similar to those found at the Carbfix site, with key minerals including K-feldspar, augite, pigeonite, and magnetite. Table 3 summarizes the molar fractions of the sample components and their respective reactive surface areas adopted. During the simulation, kinetic parameters for the dissolution and precipitation of minerals were adopted from the Carbfix.dat database.

Table 3. Molar fractions and reactive surfaces of basaltic rock minerals

Primary mineral	Mineral form	Molar fraction	Reactive surface area m^2/g
Glass Basalt	$SiTi_{0.02}Al_{0.36}Fe_{0.19}Mg_{0.28}Ca_{0.26}Na_{0.08}K_{0.008}O_{3.364}$	45%	0.0467
K-feldspar	$KA_1Si_3O_8$	35%	0.015
Augite	$Mg_{0.45}Fe_{0.275}Ca_{0.275}SiO_3$	16%	2.7523e-02
Pigeonite	$Ca_{1.14}Fe_{0.64}Mg_{0.22}Si_2O_6$	3%	1.0873e-02
Magnetite	Fe_3O_4	1%	3.5122e-03

The simulation routine employed in this study includes the dissolution of minerals and secondary phases and the precipitation of carbonates, simulating a batch reactor process. As supercritical CO_2 is the preferred choice for CO_2 storage, based on higher density compared to gaseous CO_2, this work simulated aqueous-phase basalt- CO_2 interaction at a CO_2 pressure of 100 bar, temperatures of 40 °C and initial pH of 7.5 [17]. Based on experimental data from the site, the saturation fluid for the simulated sample, shown in Table 4, was taken from the initial composition of the formation water at the Carbfix site before CO_2 injection.

Table 4. Composition of saturation fluid

Components	Mol/kgw	Components	Mol/kgw
Cl	3e-4	Fe	1.2e-6
Si	2e-4	Al	1e-6
Ca	6e-4	$S(SO_4^{2-})$	1e-4
Mg	2e-5	Alkalinity (HCO_3^-)	2e-3
Na	1e-3	Log(O2)	-10.68
K	1e-4		

3 Results and discussion

3.1 Validation of the benchmark model

The simulations of basalt dissolution and carbonate rock precipitation using the batch reactor procedure aim to develop and validate a script model for direct use in PHREEQC to model the mineralization in host rock. The results were validated by comparing the precipitated volume fraction along the basalt after reacting for 4000 years at 40 °C, 7.5 pH, and a pressure of 100 bars. Figure 1 demonstrates the capability of the model to capture the variation in mineral carbonation volume along basalt accurately.

Initially, the reservoir pH is very low due to the injected CO_2. Compared to calcite and magnesite, siderite is preferentially formed under these low pH conditions despite comparable amounts of available Ca^{2+}, Mg^{2+}, and Fe^{2+}. According to the numerical results, siderite is identified as the predominant carbonate mineral in basalt after reacting in water equilibrated with 100 bars of CO_2 at 40 °C, which is in excellent agreement with the results reported by Pham et al. 2012 [17]

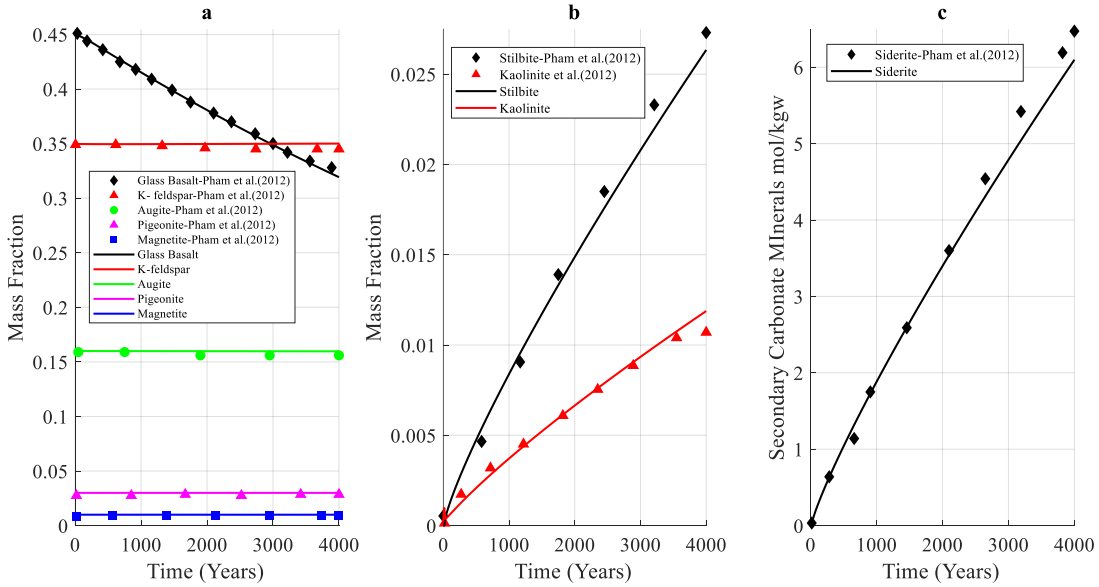

Figure 1. Basalt dissolution simulated at 40 °C and 100 bars pressure: a) Mass fraction changes of primary mineral; b) Secondary phases formed; c) Moles of carbonates formed

3.2 Sensitivity analysis

The sensitivity analysis investigates the influence of the temperature, partial pressure CO_2, and porosity in the mineral dissolution/precipitation rates. The parameters were varied one by one individually, keeping the predetermined conditions constant to observe the corresponding changes in the results. The default parameters adopted in this analysis are based on the validation conditions: 40°C temperature, 100 bars CO_2 pressure, and pH 7.5. The results that are presented and discussed focus on three main aspects: (i) the dissolution of minerals, especially for Basalt Glass, which shows the highest dissolution rate and molar fraction changes, and also for augite represents the second highest dissolution rate (Figure 2a); (ii) precipitation of carbonates, particularly siderite, identified as the predominant carbonate mineral in the basalt dissolution process (Figure 2b); and (iii) the

observed variations in pH corresponding to changes in each analyzed parameter, highlighting pH as a critical factor controlling the reactive conditions (Figure 2c).

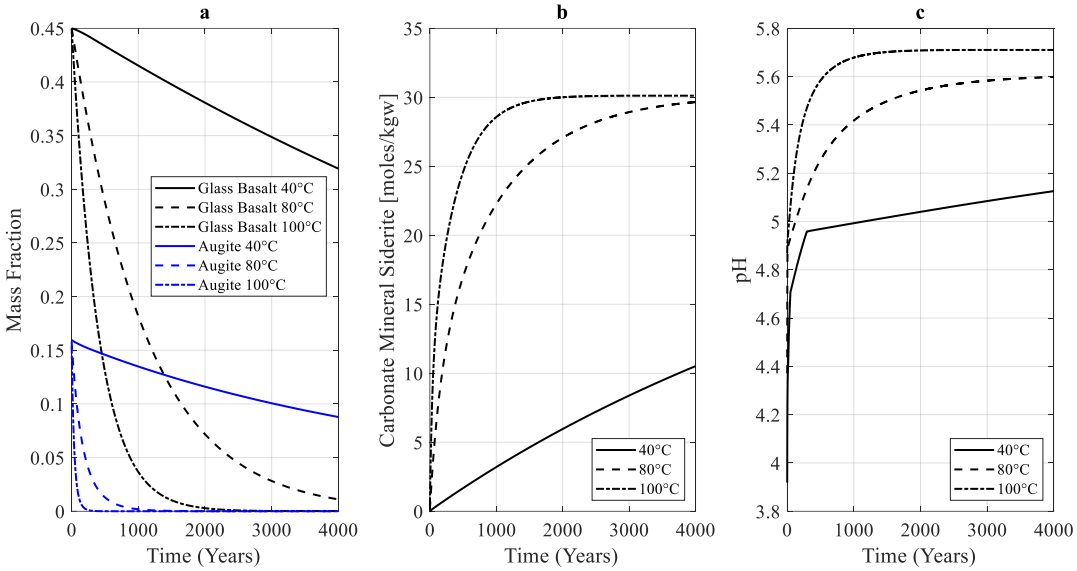

Figure 2. Influence of temperature alteration (40 °C, 80 °C, and 100 °C) on a) Fraction mass changes of minerals, b) Moles of carbonate formed, and c) pH variation.

The impact of temperature on basalt hydration and carbonation was studied by simulating the system at 80 °C and 100 °C (Figure 2), reflecting CO_2 injection at greater depths where temperatures are elevated. Dissolution rates of basalt components increase exponentially with temperature. At 80 °C, Basalt Glass is almost entirely dissolved after 4,000 years, while at 100 °C, complete dissolution takes 2,500 years. Conversely, at 80 °C, augite is completely dissolved after 1,500 years, whereas at 100 °C, complete dissolution takes less than 500 years. Thus, elevated temperatures in deeper formations would significantly accelerate mineralization. Figure 2b indicates the increased precipitation rate of carbonate minerals such as siderite with rising temperatures from 40 °C to 80 °C and 100 °C. This increase in precipitation is due to the enhanced dissolution rate of basalt, which is directly proportional to the rise in temperature, resulting in a greater quantity of divalent cations that form carbonates. Siderite minerals formed under all conditions. The formation of Fe-rich carbonates is favored by the rapid dissolution of Fe-bearing minerals like olivine and pyroxene in basalt, as noted by [18]. As basaltic rock progressively dissolves, the pH increases, and the dissolved CO_2 decreases due to the formation of Fe-rich carbonates, Figure 2c. At higher pH levels, carbonates become more prevalent, forming minerals such as siderite and solid solutions.

The simulation adopted a batch reaction type similar to a closed system in relation to CO_2, where the total inorganic carbon (TIC) is known and constant. The CO_2-driven decrease in pH, associated with the dissolution of large amounts of CO_2, initially increases the solubility of carbonates for less than 50 years, continuing to increase at a slower rate up to 300 years. After 300 years, the pH tends to stabilize (see Figure 3). Basaltic mineral dissolution is just the first step in mineral carbonation, which provides the divalent cations (Ca^{2+}, Fe^{2+}, Mg^{2+}) needed to form Ca-bearing carbonates. The dissolution of basalt is significantly affected by these pH changes, requiring a more significant amount of basalt dissolution to achieve mineral carbonation. The alkalinity produced in the reactor is insufficient to overcome the buffering capacity of carbonic acid and achieve carbonate saturation. In a closed system, the buffering capacity stabilizes significant pH variations after 300 years, as shown in Figure 3c. Then, it is expected that the basalt dissolution and carbonate precipitation rates will not be significantly affected by the variation in CO_2 pressure applied in the batch reactor, which is equivalent to a closed system.

The increase in porosity changes the rock-fluid interphase area, which implies an increase in the dissolution rate of basalt minerals, especially glass basalt and augite, as shown in Figure 4. For Glass Basalt, adopting 10% porosity resulted in dissolution of up to a mass fraction of 0.32 after 4000 years; with 20 % porosity, the dissolution mass fraction obtained is 0.20. Similarly, the behavior of the augite dissolution rate increases as a function of the increase in porosity. For 10 % porosity, dissolution of a mass fraction of up to 0.087 was obtained after 4000 years; with 20 % porosity, the dissolution mass fraction obtained is 0.047 (see Figure 4a).

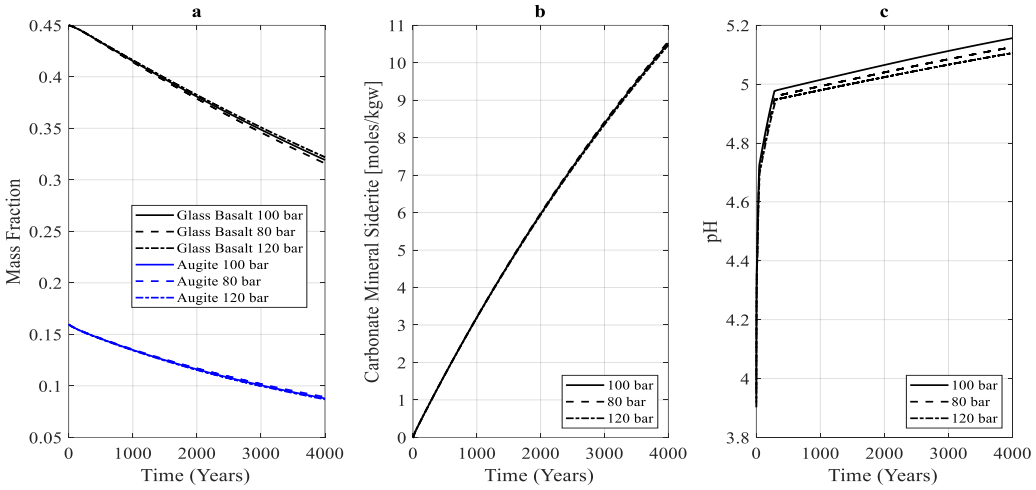

Figure 3. Influence of CO_2 pressure variation (100 bars, 80 bars, and 120 bars) on a) Fraction mass changes of minerals, b) Moles of carbonate formed, and c) pH variation.

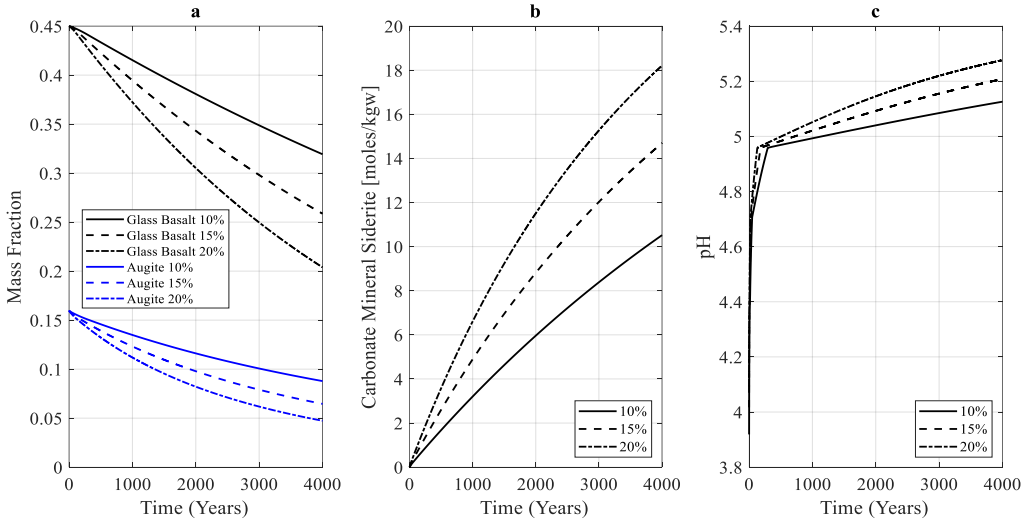

Figure 4. Influence of porosity variation (10 %, 15%, and 20%) on a) Fraction mass changes of minerals, b) Moles of carbonate formed, and c) pH variation.

Increasing the surface area of basalt results in a greater release of divalent cations, mainly Fe^{2+}, in the beginning of the dissolution and a smaller quantity of Ca^{2+} and Mg^{2+} after several decades. This divalent cation contributes to the formation of carbonates. Figure 4b shows an increase in the formation of iron-rich carbonates, siderite. For 20 % porosity, the amount of siderite obtained is approximately 1.7 times greater. Finally, the variation in pH can be explained by the increase in the reaction rate, which reduces the concentration of H^+ in the solution and makes the medium more basic as the applied porosity increases, as shown in Figure 4c.

4 Conclusions and Future work

The sensitivity analysis of the parameters is a necessary step for a better understanding of the effects of the studied parameters on the problem of basalt mineral dissolution and carbonates precipitation. This study demonstrates its practical applicability in real-world scenarios, particularly in the field, as well as in experimental settings. In practical applications, it helps idetermining the optimal depth or layer as target for injecting CO_2, significantly enhancing the reactive rate of minerals. By precisely targeting the most effective layers, this approach can maximize CO_2 mineralization, leading to more efficient carbon sequestration operations. On the experimental side, it aids in defining the settings by identifying key parameters and their impacts, enabling more precise and effective experiment design. This dual applicability ensures that the insights gained are valuable for both practical implementations and the development of robust experimental protocols.

It can be concluded that the increase in temperature is directly proportional to the increase in the reactive rate of minerals and the increase in precipitated carbonates, promising greater CO_2 mineralization with rising temperatures. This temperature rise accompanies increasing depth, driven by the geothermal gradient, which leads to higher temperatures at greater depths, further enhancing the reactivity of minerals and CO_2 sequestration. The study demonstrates that the reactive surface area influences basalt dissolution, leading to increased carbonate precipitation. Near the injection well, low pH and high CO_2 enhance permeability and porosity, but higher pH and lower CO_2 can reduce carbonate formation by consuming ions and pore space. For optimal carbon mineralization, fresh, porous rocks are preferred, and controlling the injection rate to maintain low pH near the well helps maximize CO_2 storage and minimize mineral buildup. Through sensitivity analysis of CO_2 pressure, it has been shown that in experimental settings, the applied CO_2 pressure in a closed system and the salinity of the injection fluid create a buffering effect that prevents abrupt pH changes. Consequently, variations in pCO_2 have minimal impact on the results, making other parameters such as temperature and porosity more significant in the batch experimental context.

Moreover, this study successfully validated the analyses of a basalt sample that is not from the Carbfix site, utilizing the carbfix.edu library. This promising outcome encourages further investigation into a diverse range of samples, with future research planned to include Brazilian samples. Such an expansion will enhance the scope and applicability of the findings, establishing a more robust foundation for future research and practical applications.

Acknowledgements. The authors gratefully acknowledge Fundação Carlos Chagas Filho de Amparo à Pesquisa do Estado de Rio de Janeiro (FAPERJ) under process CNE2022 E-26/200.463/2023 and Conselho Nacional de Desenvolvimento Científico e Tecnológico (CNPq) under process PQ 315077/2023-9.

Authorship statement. The authors hereby confirm that they are the sole liable persons responsible for the authorship of this work, and that all material that has been herein included as part of the present paper is either the property (and authorship) of the authors, or has the permission of the owners to be included here.

References

[1] X. Sun, Y. Bi, Y. Guo, M. Ghadiri, and S. Mohammadinia, "CO2 geo-sequestration modeling study for contact angle estimation in ternary systems of brine, CO2, and mineral," *J. Clean. Prod.*, vol. 283, p. 124662, 2021, doi: 10.1016/j.jclepro.2020.124662.

[2] H. Wu, R. S. Jayne, R. J. Bodnar, and R. M. Pollyea, "Simulation of CO2 mineral trapping and permeability alteration in fractured basalt: Implications for geologic carbon sequestration in mafic reservoirs," *Int. J. Greenh. Gas Control*, vol. 109, no. May, p. 103383, 2021, doi: 10.1016/j.ijggc.2021.103383.

[3] A. N. Awolayo, C. T. Laureijs, J. Byng, A. J. Luhmann, R. Lauer, and B. M. Tutolo, "Mineral surface area accessibility and sensitivity constraints on carbon mineralization in basaltic aquifers," *Geochim. Cosmochim. Acta*, vol. 334, pp. 293–315, 2022, doi: 10.1016/j.gca.2022.08.011.

[4] A. Raza, G. Glatz, R. Gholami, M. Mahmoud, and S. Alafnan, "Carbon mineralization and geological storage of CO2 in basalt: Mechanisms and technical challenges," *Earth-Science Reviews*, vol. 229. Elsevier B.V., Jun. 01, 2022. doi: 10.1016/j.earscirev.2022.104036.

[5] A. H. Assen, Y. Belmabkhout, K. Adil, A. Lachehab, H. Hassoune, and H. Aggarwal, "Advances on CO2 storage. Synthetic porous solids, mineralization and alternative solutions," *Chem. Eng. J.*, vol. 419, no. November 2020, p. 129569, 2021, doi: 10.1016/j.cej.2021.129569.

[6] H. J. Ho and A. Iizuka, "Mineral carbonation using seawater for CO2 sequestration and utilization: A review," *Sep. Purif. Technol.*, vol. 307, no. November 2022, p. 122855, 2023, doi: 10.1016/j.seppur.2022.122855.

[7] C. Marieni, M. Voigt, D. E. Clark, S. R. Gíslason, and E. H. Oelkers, "Mineralization potential of water-dissolved CO2 and H2S injected into basalts as function of temperature: Freshwater versus Seawater," *Int. J. Greenh. Gas Control*, vol. 109, Jul. 2021, doi: 10.1016/j.ijggc.2021.103357.

[8] S. Delerce, P. Bénézeth, J. Schott, and E. H. Oelkers, "The dissolution rates of naturally altered basalts at pH 3 and 120 °C: Implications for the in-situ mineralization of CO2 injected into the subsurface," *Chem. Geol.*, vol. 621, no. December 2022, p. 121353, 2023, doi: 10.1016/j.chemgeo.2023.121353.

[9] D. Wolff-Boenisch, S. Wenau, S. R. Gislason, and E. H. Oelkers, "Dissolution of basalts and peridotite in seawater, in the presence of ligands, and CO2: Implications for mineral sequestration of carbon dioxide," *Geochim. Cosmochim. Acta*, vol. 75, no. 19, pp. 5510–5525, 2011, doi: 10.1016/j.gca.2011.07.004.

[10] S. Kanakiya, L. Adam, L. Esteban, M. C. Rowe, and P. Shane, "Dissolution and secondary mineral precipitation in basalts due to reactions with carbonic acid," *J. Geophys. Res. Solid Earth*, vol. 122, no. 6, pp. 4312–4327, Jun. 2017, doi: 10.1002/2017JB014019.

[11] R. M. Pollyea and J. D. Rimstidt, "Rate equations for modeling carbon dioxide sequestration in basalt," *Appl. Geochemistry*, vol. 81, pp. 53–62, 2017, doi: 10.1016/j.apgeochem.2017.03.020.

[12] S. R. Gislason *et al.*, "Rapid solubility and mineral storage of CO2 in basalt," *Energy Procedia*, vol. 63, pp. 4561–4574, 2014, doi: 10.1016/j.egypro.2014.11.489.

[13] E. H. Oelkers, S. R. Gislason, and J. Matter, "Mineral carbonation of CO2," *Elements*, vol. 4, no. 5, pp. 333–337, 2008, doi: 10.2113/gselements.4.5.333.

[14] D. L. Parkhurst and C. A. J. Appelo, "PHREEQC Version 3 — A Computer Program for Speciation , Batch-Reaction , One-Dimensional Transport , and Inverse Geochemical," *U.S. Geol. Surv. Tech. Methods, B. 6, chapter A43*, pp. 6-43A, 2013, doi: 10.1016/0029-6554(94)90020-5.

[15] M. Heřmanská, M. J. Voigt, C. Marieni, J. Declercq, and E. H. Oelkers, "A comprehensive and internally consistent mineral dissolution rate database: Part I: Primary silicate minerals and glasses," *Chem. Geol.*, vol. 597, May 2022, doi: 10.1016/j.chemgeo.2022.120807.

[16] M. Voigt, C. Marieni, D. E. Clark, S. R. Gíslason, and E. H. Oelkers, "Evaluation and refinement of thermodynamic databases for mineral carbonation," *Energy Procedia*, vol. 146, pp. 81–91, 2018, doi: 10.1016/j.egypro.2018.07.012.

[17] T. H. Van Pham, P. Aagaard, and H. Hellevang, "On the potential for CO2 mineral storage in continental flood basalts-phreeqc batchand 1d diffusion-reaction simulations," *Carbon Capture Storage CO2 Manag. Technol.*, pp. 178–202, 2014, doi: 10.1201/b16845.

[18] S. Gudbrandsson, D. Wolff-Boenisch, S. R. Gislason, and E. H. Oelkers, "An experimental study of crystalline basalt dissolution from 2pH11 and temperatures from 5 to 75°C," *Geochim. Cosmochim. Acta*, vol. 75, no. 19, pp. 5496–5509, Oct. 2011, doi: 10.1016/j.gca.2011.06.035.